CFD MODELS FOR THE ANALYSIS OF ROTOR-ONLY INDUSTRIAL AXIAL-FLOW FANS

Massimo MASI[1], Andrea LAZZARETTO[2]

[1] *University of Padova, DTG - Department of Management and Engineering, Stradella S. Nicola 3, 36100, Vicenza, Italy*

[2] *University of Padova, Via Venezia 1, 35131, Padova, Italy*

SUMMARY

Local and total performance of an actual rotor-only axial flow industrial fan have been evaluated by experimental tests and CFD calculations. Different degrees of the overall model complexity and amplitudes of the computational domain are considered in the latter to find the best compromise between accuracy of the results and saving of computational effort and costs. All computational domains were discretised taking advantage of the innovative polyhedral grid meshing capability of CFD commercial codes. The importance of the proper grid size for scientific and industrial applications is discussed also accounting for the turbulence model selection.

Results show that single blade channel stationary calculations with an idealized meridional passage show the better predictions of the total fan performance and efficiency in the stable operation range. Reliable analysis of the rotor flow field can be performed only by modeling in detail the actual meridional geometry. In addition, calculations on a very rough grid show capability of performance and efficiency prediction that appears very attractive for fan industry.

INTRODUCTION

The actual performance of industrial fans has not yet reached the level claimed as possible by a considerable amount of up-to-date literature in which optimisation algorithms drive campaigns of CFD calculations. On one side this is due to a well-established know-how often considered as “satisfactory” by the manufacturers. On the other side there is still a lack of confidence in the technical and economic advantages deriving from time consuming optimisation techniques. However, big interest of manufacturers is devoted to effective design and analysis techniques that are compatible with the acceptable computational effort and costs in industrial production.

Thanks to the advances in computer technology, computational models suggested by researchers became an attractive scenario for fans industries.

Fundamentals of theory and analysis techniques for arbitrary-vortex flow turbomachinery are from a long time subjects of classical text-books (see e.g. [1], [2]). In the early ’60 the first digital techniques for turbomachinery analysis were developed. Meaningful examples are the streamline

curvature methods by Stockman [3] and Novak [4]. An extensive review of the state of the art up to 1980 about numerical analysis of turbomachinery internal flows is presented by McNally and Sockol [5]. This work summarizes all the relevant modelling techniques which anticipate the massive use of present powerful CFD tools. Besides the theoretical assumptions and reduction of fluid-dynamics equations suggested by pioneers of modern CFD, the authors reviewed also structured grid solutions and basic turbulence modeling, which are still the basis of most CFD software for turbomachinery analysis. Although these numerical modelling techniques appears obsolete for a detailed analysis of the internal flows, they may become a useful support to design in industrial engineering because of the enhanced capability of today's computing machines.

More recently, various optimisation techniques supported by CFD computations were suggested to aid the design of axial fans, which are claimed to provide reliable results. However, these results are often obtained at the expense of high computational effort and costs. Thus, it is common practice to perform calculations taking advantage of the periodic symmetry in azimuthal direction of bladed passages. In 2002 Lin et al. [6] improved the blade design of a high boss ratio rotor-only axial flow using an optimisation algorithm coupled to an artificial neural network (ANN). Performance estimates were obtained by CFD computations on CFX Tascflow® finite volume solver running on hexahedral structured grids. The only blade passage without tip clearance was solved using the relative reference flame calculation approach. To reduce the computational time (which is not declared by authors) for the overall optimisation process the grid was limited to 34,875 cells (75x31x15). In 2007 Li et al. [7] analysed the effectiveness of forward-skewed blading for an axial-flow fan impeller using a genetic algorithm and the EURANUS CFD solver coupled to a neural network. Still, the computations were performed on a single blade passage, taking into account tip clearance. The computational domain was meshed with 650,000 structured cells in a H-type grid, and the algebraic one equation Spalart-Allmaras turbulence model was used. Authors did not clarify the computational cost of the optimisation process, but they show numerical results that agree quite well to detailed experimental measurements. To design a multi-stage axial flow fan, in 2009 Cho et al. [8] suggested an optimisation technique based on the gradient method. The degree of freedom for the optimisation process are higher than in Li et al. [7]. Only one passage of one rotor and stator was calculated by the “frozen rotor” motion model using the CFX®-11 finite volume code to estimate aerodynamic performance. The authors declare that the results obtained by the block-structured grid used to mesh blade passages are independent of cells number when more than 200,000 cells are used to discretise the whole computational domain. The Menter SST turbulence model was used, and a target y^+ lower than 5 was assured in all computations. Numerical results showed good agreement with experimental curves trend, overestimating performance only slightly, and efficiency more heavily. Authors declared that one calculation needs 40 minutes on parallel processing calculation with four computers of Duo CPU Core 2 E8400 (3.0 GHz), being 250 the required number of calculations needed to complete the optimisation process.

On the other hand, many complex computational models supported by experimental studies are suggested in the literature to improve aerodynamic and noise performance, which focus on relevant design details of axial-fans. Recently, Corsini at al. [9] investigated the effectiveness of tip end-plates to control leakage vortices within a wider study on passive techniques for rotor tip noise control in low-speed axial-flow fans. The CFD analyses were run on an original parallel multi-grid RANS equations solver that implements variants of non-linear k-ε turbulence model. The rotating reference flame approach was applied on a grid obtained by merging two structured H-type grids. One grid is used for the main flow region surrounding the blade, the other one for the embedded mesh in the tip-gap region. The grid of the main flow region alone counts more than 600,000 cells.

All the above cited CFD models were discretised using hexahedral structured grids, being well-known the poor computation accuracy of tetrahedral grids. On the other hand, the time consuming procedures and the intrinsically high cells number involved with structured grids are penalizing aspects with unacceptable costs for extensive use of CFD at industrial level.

This paper presents a series of CFD analyses of a rotor-only axial flow fan validated on experimental tests. The first part analyses the sensitivity of numerical results to the variation of grid size and turbulence models. The results of four numerical models of different degree of detail and overall complexity are then presented and compared to total performance parameters data measured on two different fan test rigs. All computational domains were discretised taking advantage of the innovative polyhedral grid meshing capability of CFD commercial codes.

The work is the preliminary step in the development of a design procedure of rotor-only axial-fans for reliable industrial applications aimed at minimising computational time and resources in complex CFD calculations.

THE FAN

The rotor-only ducted axial fan is designed for swirl-free inlet flow conditions. The main geometrical features of the fan are shown in Table 1. Blades are mounted on the hub using a conical base that introduces a sharp variation of blade thickness.

Table 1: Main features of the fan.

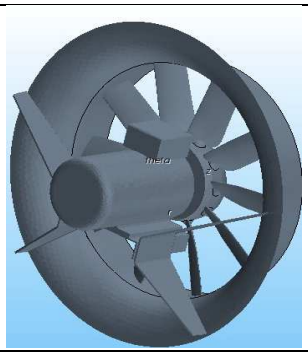

Parameter	**value**
External diameter *D*	630 mm
Boss/tip ratio	0.35
Number of blades	10
Blade design (theoretical)	forced vortex (εs=const.)
Blade thickness/chord	10%
Tip clearance/blade height	2%
Blade setting angle	30°
Nominal speed	1425 rpm

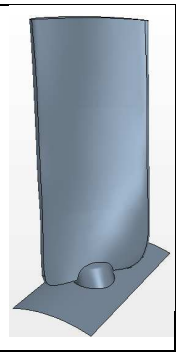

Experimental test were performed using two test rigs that were built according to the UNI10531 Standard (in agreement with ISO 5801 [10]). One of the two belongs to the B installation category (free inlet, ducted delivery), and was used for faster tests. Fan volume flow rate is evaluated using suitable orifice plates, delivery pressure is measured through pressure tappings in the duct downstream of the antiswirl element. The other test rig (belonging to category A, with plenum chamber at the inlet and free delivery) was built for more accurate tests. Venturi tube is used to measure volume flow rate, stagnation pressure is acquired in the plenum chamber. Electric consumption of the motor is measured to evaluate total fan efficiency for both the two test rig

The data were acquired by TESTO® measuring equipment mod. 452, equipped with 0638.1545 pressure probe which assures 0.5% of measured value overall accuracy. The resolution and accuracy of relative humidity sensor were 0.1 and 2% of measured value, respectively. DELTA® thermometer mod. HD2328.0 equipped with K-type thermocouples provided air temperature with 0.1°C resolution and accuracy.

Fan performance are evaluated through the non dimensional parameters flow coefficient Φ, total pressure coefficient ψ and total efficiency η, which write:

$$\Phi = \frac{Q_v}{\omega D^3} \qquad \Psi = \frac{p_t / \rho}{(\omega D)^2} \qquad \eta = \frac{p_t Q_v}{P_m} \qquad (1),$$

where Q_v is volume flow rate, p_t is fan total pressure, P_m is mechanical power at rotor shaft, ω and D are angular velocity and diameter of fan, respectively.

Fan total pressure is defined as:

$$p_t = p_s + \frac{\rho}{2}\left(\frac{Q_v}{A}\right)^2 \qquad (2).$$

where ρ is the mass density of fluid, p_s the fan static pressure and A the fan outlet section.

GENERAL CONSIDERATIONS ABOUT GRIDS

An inherent problem of structured grids derives from the high number of cells in every zone of the domain, both where they are needed to capture local effects and where they are not, with a consequent "waste" of calculation resources.

In this work the mesh is built using a non structured polyhedral grid. Compared to a structured hexahedral grid the degree of accuracy is slightly lower at fixed number of cells, but calculation resources can be saved using a higher detail only where needed. On the other hand, compared to traditional tetrahedral non structured grids the accuracy on physical quantities in a cell is considerably improved by the higher number of adjacent cells (often greater than 10). That is why these grids supply reliable results also in the analysis of complex domains, and demonstrate to be suitable for industrial applications where the time available for calculations is often limited. All calculations were performed using the CD-Adapco® CFD software STAR-CCM+ v6.02.009.

To reduce computational effort it is common practice in blade rows calculation to accept solutions obtained by exploiting the azimuthal periodicity. Using this option, polyhedral grid provide the further possibility of increasing the grid level of detail on annular sectors limited by plane periodic surfaces that may also intersect solid parts. Instead, a block structured approach imposes periodic surfaces along azimuthal directions, which are often very complex depending on blading characteristics. In fact, to facilitate the structured grid construction, lateral surfaces at the same azimuthal level are used upstream and downstream of the blade, whereas around the blade these surfaces have radial generatrix which approximately follows the blade profile average line. Commercial software packages are available in the market that include additional modules aimed at reducing the time for grid construction. However, their use is to be carefully considered due to high costs for purchase and learning, which are often not justified at industrial level.

GEOMETRICAL DOMAINS AND COMPUTATIONAL GRIDS

Various approximations were introduced in the numerical models that were built to simulate the flow field within the fan. Only one of the ten blade passages is modeled assuming that the geometrical features of machine and ancillary components remain periodically the same as it is for the rotor blading. This hypothesis is common to the three first domains analyzed here, the latter featuring real geometrical characteristics. All these domains are briefly described in the following.

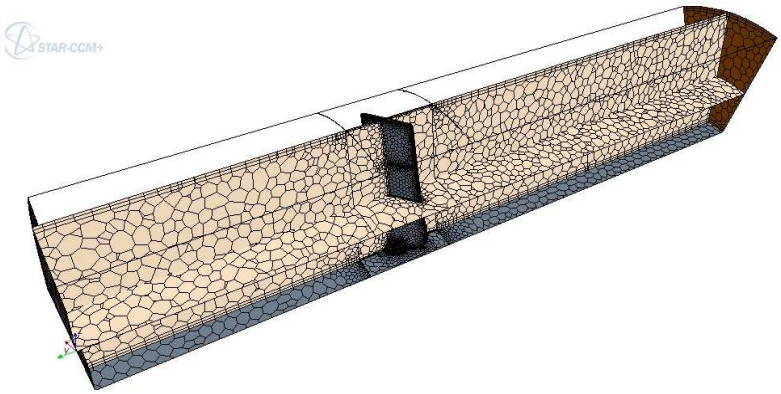

Figure1: Model M1 domain sections and boundary surfaces (37,000 cells within the fluid volume enclosing rotor).

Model 1 (M1)

This geometrical domain includes a meridional rectilinear duct with no clearance between blade tip and external containing duct (see Figure 1). Inlet is set 4 chord lengths upstream of the rotor (400mm upstream of blade nose). So, the absolute velocity vectors can be reasonably assumed to be perpendicular to the inlet surface. Domain exit is set 6 chord lengths downstream of the blading (approximately 600mm downstream of blade tail) in order for the blade wakes to be closed.

Model 2 (M2)

This geometrical domain substantially coincides with M1, the only difference being the clearance between blade tip and casing. Beside the meshed surfaces in Sub-figure 2 (left) show a meridional section and two circumferential planes which limit the volume conventionally indicated as "rotor volume". Sub-figure 2 (left middle) shows a detail of the geometrical model around the blade tip.

Model 3 (M3)

The meridional geometry is modified in this model in order to be closer to the real one (Sub-figures 2 right). The electric motor set upstream of the rotor and the bell-mouth entry provided to facilitate the air flowing towards the machine are included. Cross section of the plenum chamber is much bigger than that of the fan delivery section in order to agree with test rigs dimensions defined by UNI 10351 Standard [10].

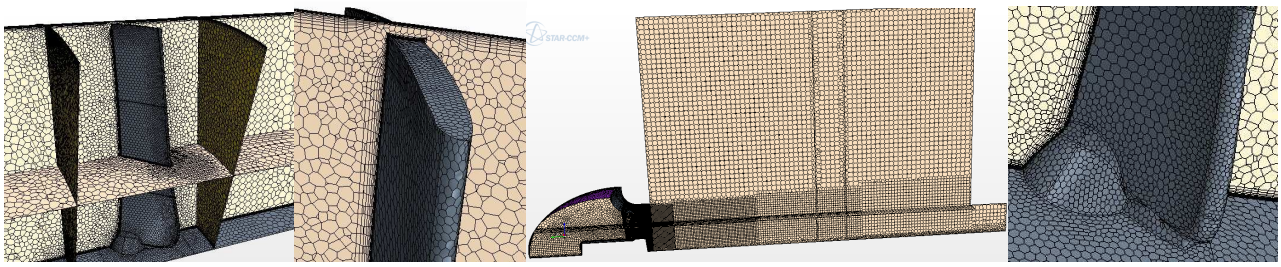

Figure 2. Model M2 domain sections and boundary surfaces (left) and tip clearance detail (left middle). Model M3 domain sections and boundary surfaces (middle right), and blade root detail (right).

Model 4 (M4)

Starting from an opposite idea to the search of the detail, a very rough grid was built in this model, which is able to include all elements that were neglected in the previous models (Figure 3). The domain describes the assembly presented above (for M3) with the inclusion of motor supports and electric cable box which were neglected by all previous models.

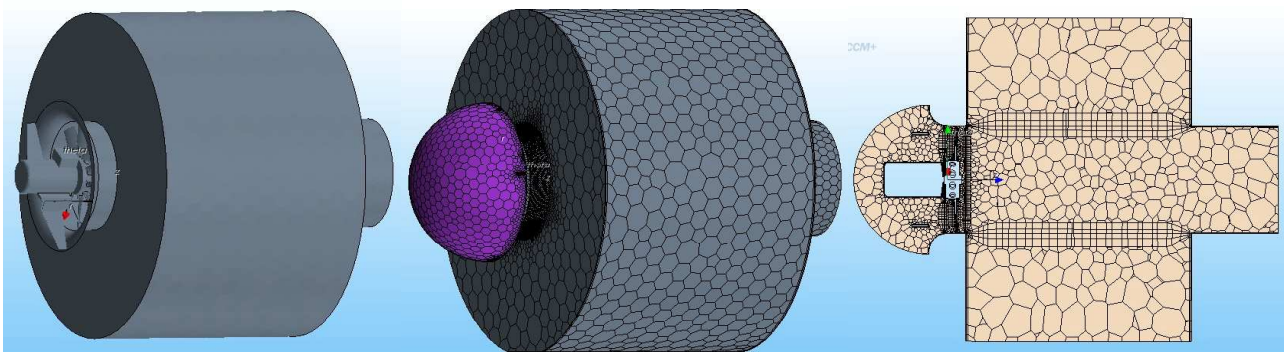

Figure 3. Model M4 – geometry (left), domain surface mesh (middle) and whole grid section (right).

PHYSICAL AND NUMERICAL MODELS

Fluid is modelled as incompressible air due to the fan low pressure ratio (density and dynamic viscosity are kept constant to value ρ = 1.226 kg/m^3 and μ =1.78 10^{-5} Pa s, respectivly).

Boundary conditions pairs imposed at inlet/outlet surfaces pair were mass-flow inlet/pressure outlet and total pressure/mass-flow outlet in models 1-2 and 3-4, respectively. Models 1, 2, and 3 featured periodic and slip-wall conditions at azimuthal and inner/outer radial boundaries, respectively, if present. All the solid surfaces (blading, hub, casing, motor, etc.) were modeled as smooth walls.

In all simulations Reynolds equations are "closed" using different type of two-equations k-ε algebraic model. Uniform turbulence intensity (1.5%) and length scale (90mm), respectively, were imposed at the inflow section of all models. As explained in the following specific sections, standard log-law wall function was used for the grid sensitivity analysis, whereas shear driven Wolfstein [12] near wall treatment was used for turbulence model sensitivity analysis and for final calculations when both near wall grid density and wall y^+ were in the proper range. Table 2 shows the main physical and numerical characteristics of the four models used in the final calculations.

The steady-state calculations (models M1, M2 and M3) were considered to converge when the monitored local and total parameters do not change with iterations and all the normalized residuals of scalar equations solved become lower than 10^{-4}. Time step used in model M4B correspond to 3deg of rotor motion. Models M4 calculations were interrupted when fan performance parameters and other local fluid-dynamics monitors showed constant or periodically repeating values.

Table 2: Main characteristics of the present models

	Model 1	**Model 2**	**Model 3**	**Model 4 A / B**
Turbulence	Realizable k-ε two-layer [11]			
Motion model	Stationary relative reference frame			Stationary multi-reference-frame / moving mesh
Solver	Steady Segregated			Steady / Unsteady Segregated
Advection	2nd order upwind			
Time scheme	-			- / 1st order Euler implicit
Algorithm	SIMPLE-type			
Computation time	20hr (CPU i5-2430m 2.4GHz)		24hr (CPU i5-2430m 2.4GHz)	4 / 30hr (CPU Pentium 1.6GHz)

GRID SENSITIVITY ANALYSIS FOR MODEL 1

The search for mesh independent conditions is not an easy task, depending not only on the quantities involved but also on the choices of physical models and numerical schemes. This search is performed considering:

a) Parameters of performance of the entire machine, i.e. total pressure and efficiency, in order to find the minimum number of cells required to evaluate the overall fan performance;

b) Lift and drag coefficients of the blade sections approximately located at one-third and two-thirds of blade span (i.e. at radii 170mm and 250mm), in order to find the minimum number of cells required to evaluate local blading performance.

The analysis was performed using M1 because it offers the highest detail at fixed cell number. Operation conditions are: maximum efficiency, rotational speed n = 1425 rpm; volumetric flow rate Qv = 4.2288 m^3/s. A prism sub-layer is used in all calculations. The domain is sub-divided into three regions: upstream, rotor and downstream. In the upstream and downstream regions the number of cells was kept approximately constant under the assumption of well uniform and

distributed motion. The grid is instead progressively refined close to the rotating region to make the reduction in cells dimension progressively higher.

The first series of simulation runs was aimed at evaluating the sensitivity of model results to grid size. Physical models, numerical schemes and target wall y^+ were kept the same in all runs, while progressively refining the mesh at each step by increasing its density of a factor 8. Accordingly, the spatial level of detail is doubled in two successive runs. Thus, starting from a rough grid of about 7,500 cells, three successive refinements of 37,000, 300,000 and 2,250,000 cells within rotor fluid volume, has been tested, respectively. The Standard k-ε turbulence model including the standard log-law wall function was used. The 2-cells prism sub-layer keeps the value of wall y^+ close to 30.

Figure 4 compares the results for various grid refinements. Diamond and square markers connected by dotted lines are referred to successive refinements discussed above and indicate local aerodynamic parameters (a and b) and total performance parameters (c and d), respectively. The reference sections used for total performance parameters calculations were places 25mm upstream and downstream to volume swept by rotor blading. Both these parameters show the expected asymptotic trend. It is apparent at a glance that the first two grids (7,500 and 37,000 cells) are not sufficiently dense, whereas the last one (225,000 cells) is certainly too dense due to the long calculation time required (48 hours on 4 threads INTEL® i5-2430m 2.4GHz CPU). But appreciable differences can still be observed comparing the solutions obtained using 300,000 and 225,000 cells. So, an additional series of simulation runs were performed using intermediate numbers of cells (450,000, 610,000, 810,000, 1,200,000). The results are show by circle markers in Figure 4.

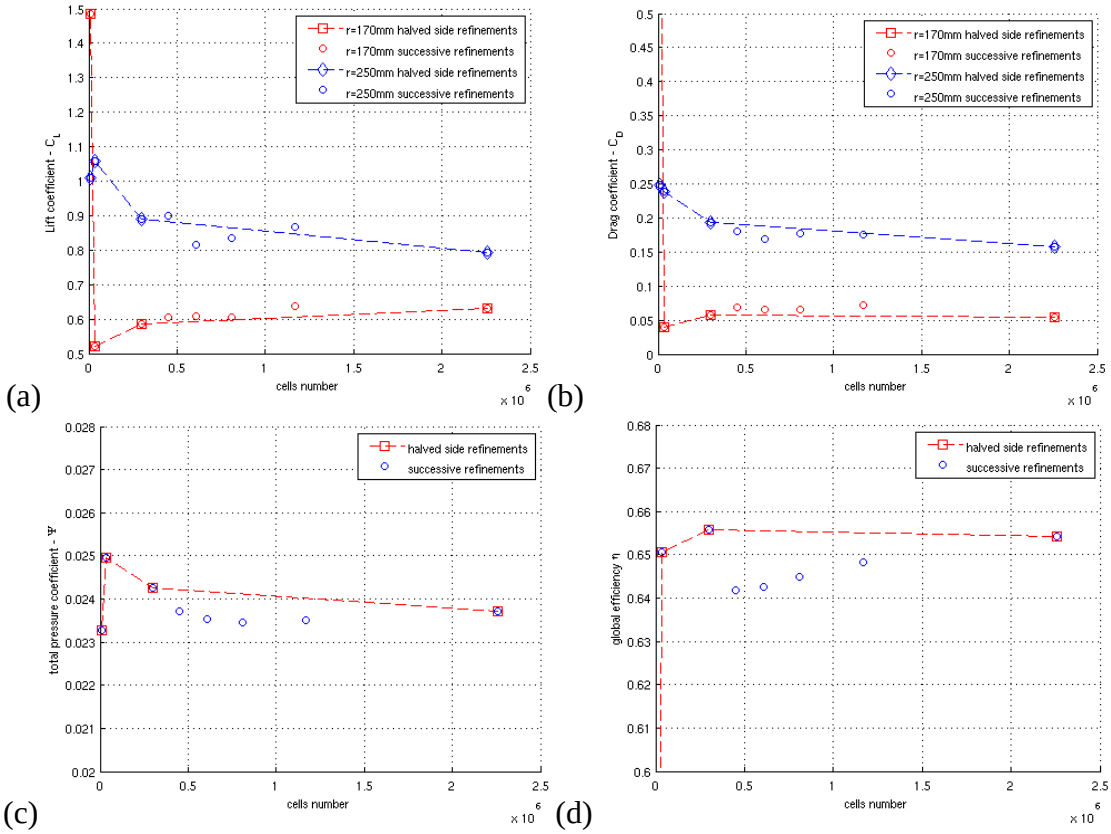

Figure 4. Profile lift (a) and drag(b) coefficients, total pressure coefficient (c) end efficiency (d) against cells number in the rotor volume

These intermediate runs show that the trend of the performance quantities is not properly asymptotic and that the 2,250,000 cell case cannot strictly be declared independent of a further increase in the cell number. However, it appears that above 610,000 cells in the rotor blade channel the variations of all performance parameters is quite small, with the only exception of the total fan efficiency. These variations are considered acceptable for the scope of the present analysis so that

the 610,000 cells grid is considered the limit beyond which results are independent of grid dimension. On the other hand, the still significant variations of the total fan efficiency beyond 610,000 cells indicate the need for further increases in the number of cells in the zone downstream of the rotor in which the flow undergoes frictional losses generated by strong non-uniformity.

TURBULENCE MODEL SENSITIVITY ANALYSIS FOR MODEL 1

Simulation results obtained for Model 1 using the Standard k-ε turbulence model are compared in Figure 5 with those obtained with Realizable k-ε and two-layer Realizable k-ε models. The comparison is limited to meshes including 450,000 610,000 and 810,000 cells. Performance parameters obtained using Realizable k-ε model of Shih [11] are always lower than those obtained with the k-ε Standard model, the more significant differences being associated with total fan efficiency. The Wolfstein [12] near-wall low-Reynolds sub-model was considered to further enhance the solution accuracy of non-linear k-ε thanks to its more sophisticated calculation procedure close to the wall. Thus, in the two-layer Realizable k-ε calculations the prism sub-layer close to the wall was modified in comparison with the two previous cases. The overall thickness of 3mm was obtained for the sub-layer grid, which is made up of 12 cell layers in which the ratio between the thickness of two adjacent cells is 1.3. Thus the cells height close to the wall were considerably reduced (up to one tenth of millimeter) to get y+ values close to the unit (or, in any case, lower than 10). Because of this local grid refinement the total number of cells in the rotor volume has increased up 690,000, 910,000 e 1,150,000.

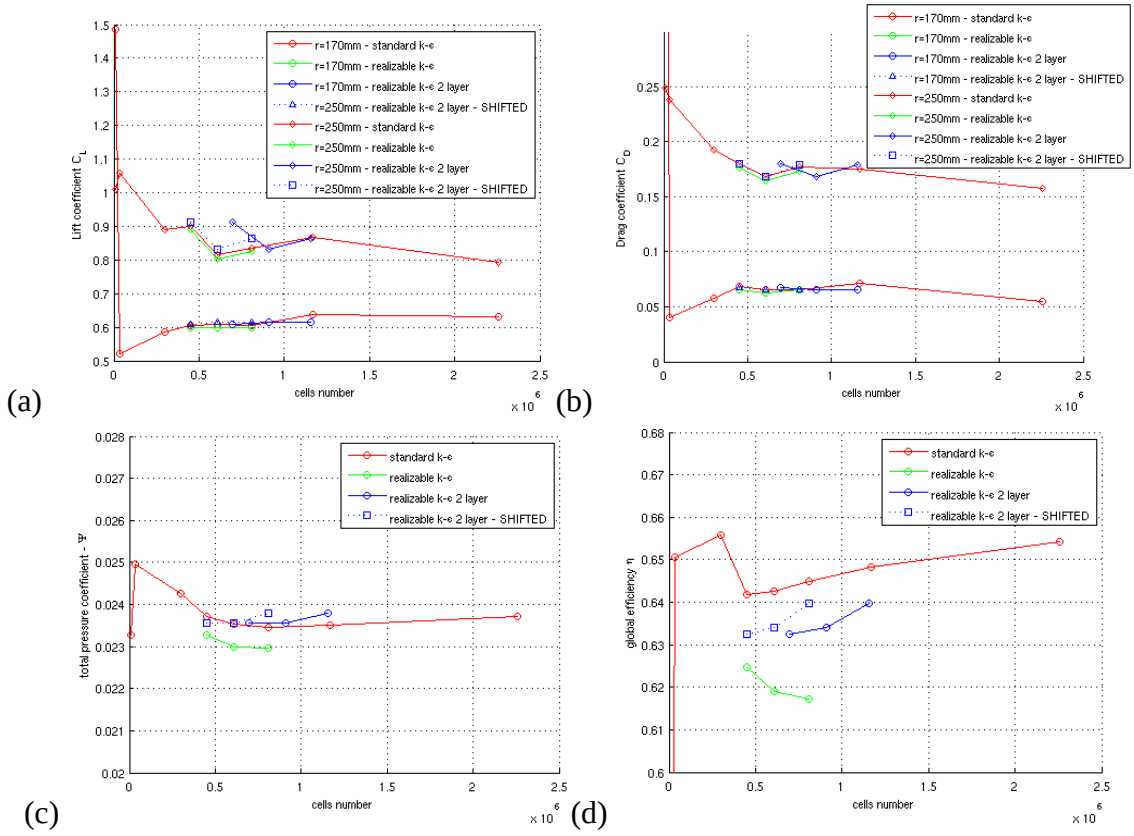

Figure 5. Local lift (a) and drag(b) blade section coefficients, total pressure coefficient (c) and total efficiency (d) for different turbulence models against cells number in the rotor volume

As it appears from Figure 5a-b, the trend of the lift and drag profile coefficients appears to be quite different from the two previous cases (diamond markers connected by blue lines). However, by neglecting the above mentioned increase in the number of cells close to the wall, and associating the results with the cells number of previous calculations having the same cells number within the blade

channel core (square markers connected by blue dotted lines), the trend are very similar to the previous cases, although lift and drag profile coefficients are higher at higher radius and lower at lower radius.

In conclusion, an increase in the accuracy of the turbulence modelling does not result in significant variations of the local aerodynamic performance parameters, whereas it has a more important influence on the total performance parameters and, in particular, on the total fan efficiency (see Figure 5c). On the other hand, we expect that the influence on the aeraulic efficiency is not important because of the similar aerodynamic local performance, while it is significant on the dissipations within fluid volumes upstream and downstream of the blade channel.

Table 3 summarises the main features of the computational grids selected for the models after the grid and turbulence model sensitivity analyses.

Table 3: Main data of the different mesh models

Region	**Model 1**	**Model 2**	**Model 3**	**Model 4 A / B**
Upstream rotor	30,000	41,000	37,000	35,000
Rotor	910,000	893,000	900,000	238,000
Downstream rotor	70,000	96,000	263,000	34,000
Total	1,010,000	1,030,000	1,200,000	307,000
prism wall layers	12	12	12	2
Rotor walls y^+	<10	<10	<10	<80

COMPARISON BETWEEN MODELS AND EXPERIMENTS

A series of simulation runs were performed to explore the performance predictive capability of the presented numerical models. The two-layer Realizable k-ε turbulence model was selected in all simulation runs. The implemented version of this model includes a check on the local wall y^+ value, which automatically switch to the Realizable k-ε if the near wall grid is not refined enough. This happens in Models 4A and 4B because of the bigger cells dimensions near wall boundaries.

Figure 6 compares the non-dimensional performance and total fan efficiency predicted by the five models to measured data. The black triangle marker indicates the design condition predicted by M1, i.e. the performance of an ideal rotor without tip clearance and any other loss due to inlet and hub characteristics, electric motor and other ancillary components. The triangular markers connected by a blue line indicate the performance curve obtained by M2. The drops in the design value of the total pressure coefficient and efficiency compared to M1 are about 7% and 4%, respectively. These losses appears to be only slightly overestimated with respect to the experimental measures by Kahane [13], whereas they are almost twice as much those suggested by Wallis [14]. It is worth noting that total performance predictions by M2 in the range of fan stable operation remain between the two experimental test rig measurements, despite its still high degree of idealization. On the other hand, the prediction in the unstable zone operation is apparently not reliable.

Instead, Model M3, which was expected to provide a more realistic approximation of the actual fan behavior, underestimates both performance and efficiency. However, M3 captures better than M2 the maximum total pressure and maximum efficiency flow rate values when referring to the experimental results obtained by the test rig of category A, which are expected to be the more reliable ones.

The rough grid approach of the multi-reference-frame model M4A (squared markers) supplies a total pressure coefficient even more underestimated than that provided by M3, being the performance curve trend of the two models very similar in the stable range of fan operation. On the other hand, the performance predictions in the unstable operation zone agree quite well to the experimental data measured in the test rig B. Moreover, M4A provides better estimates of fan

efficiency than M3 in the whole operation range covered by experimental measurements, and the efficiency curve around nominal flow rate almost overlaps the M2 estimates.

Finally, the M4B moving meshes approach improves the performance prediction obtained by M4A, so that the same underestimation level of M3 in the stable operation zone is achieved. The fan efficiency estimate of M4B agrees quite well with measurements of test rig A within the whole flow rate range.

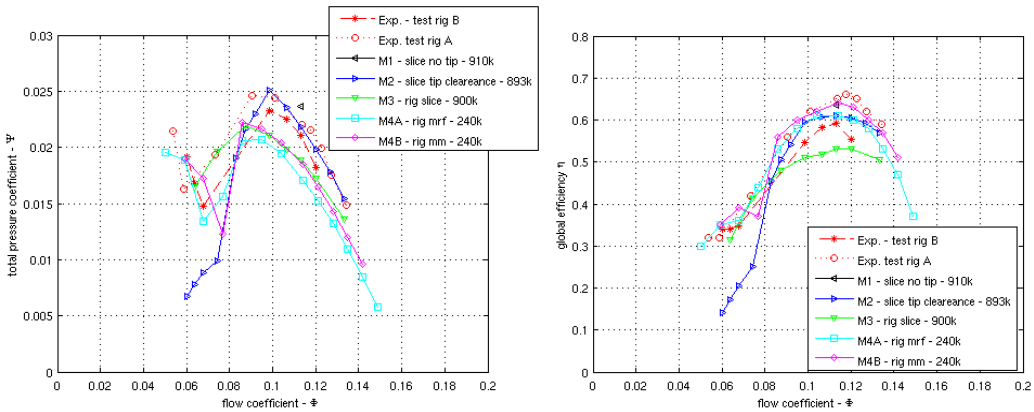

Figure6. Comparison of calculated and measured Fan total pressure (left) and efficiency (right)

CRITICAL COMPARISON BETWEEN MODELS

Figures 7 (left) and 7 (middle) show the tangential and axial velocity ratios (εs and Σa) along the non dimensional radial coordinate *x* (local/tip radii) one-quarter blade chord downstream of the rotor blading resulting by M2 and M3 calculations both at maximum efficiency flow rate. Velocity values are divided by the upstream rotor blading axial velocity to make them non-dimensional. M4B velocity distribution, which is not shown for brevity, proves to be smoother than M2 and M3 ones due to the averaging forced by grid coarseness. Despite the satisfactory prediction of total performance parameters by model M4, sometimes even better than those by M2 and M3, it is worth noting that the local features of the flow field around the rotor blading are not suited for design detailed analyses. In fact, the high tangential velocity ratio combined to the low axial velocity ratio in the near tip region predicted by M2, clearly suggests the aerodynamic stall of near tip blading profiles. The undulation of the axial velocity ratio just away from rotor hub, provided by M2 is an evidence of the wake flow due to the flow blockage induced by the conical pin which staggers the blades to the hub, as well. The roughness of the M4 grid gives less clear indications about these occurrences. On the other hand, electric motor and ancillary components prove to modify quite significantly the local velocity distribution across rotor blading. In fact, the axial velocity distribution calculated by M3 shows a shift of the through flow towards higher radial position. This occurrence, also captured by M4, moves the stall of the blade tip towards lower flow rates because of the higher axial velocity around the tip region which drives to more favourable incidence angles.

Finally, it is worth nothing axial velocity modifications within the annulus upstream of rotor blading due to interference of motor and bell-mouth entry. In fact, Figure 7 (right) shows axial velocity ratios one-third blade chord upstream of rotor blading which results from M2 and M3 calculations. It is apparent that the arbitrary vortex rotor blading design hypothesis suggested by many authors (see, e.g. Downie et al. [15]), which states the uniform distribution of axial velocity in the annulus before rotor blading, is actually not strictly verified, in particular when upstream rotor components like motor or bell-mouth entry are taken into consideration.

In summary, if we assign a “scientific computational index” equal to 100 to the computational effort required by one calculation at research level (i.e. more than 1,500,000 cells) in looking for the best trade-off between model accuracy and overall complexity, we can conclude as follows.

- Model M1 does not match industrial requirements. In fact, the computational cost appears to be disproportionate to the level of agreement with measured data. Thus, M1 looks unsuitable both for detailed analyses and preliminary design, even if the results obtained using less refined grids that reduce up to 40% the computational cost may be considered acceptable.

- Model M2 can be applied in the last design step before fan prototyping because of the reliable estimates of fan performance and efficiency in the operation range around best efficiency point at 40% of the scientific computational index.

- Model M3 is the best suited to detailed blading analysis because of the reliable computation of local flow field at 50% of the scientific computational index. However, it cannot be suggested in fan performance analysis because of the significant underestimation of experimental data. Moreover, due to the high computational cost, M3 application to optimization techniques has to be limited to the improvement of design details of existing solutions which have already reached satisfactory performance.

- On the other hand, optimisation techniques aimed at maximising fan performance in the whole operation range may take advantage of the quicker M4A response in predicting the overall range of fan operation (about 17% of the scientific computational index).

- Model M4B appears suited to support the preliminary design step in the exploration of new design potentialities. In fact, each fan operating condition along the characteristic curve is calculated in good agreement with experimental data at about 10% of the scientific computational index.

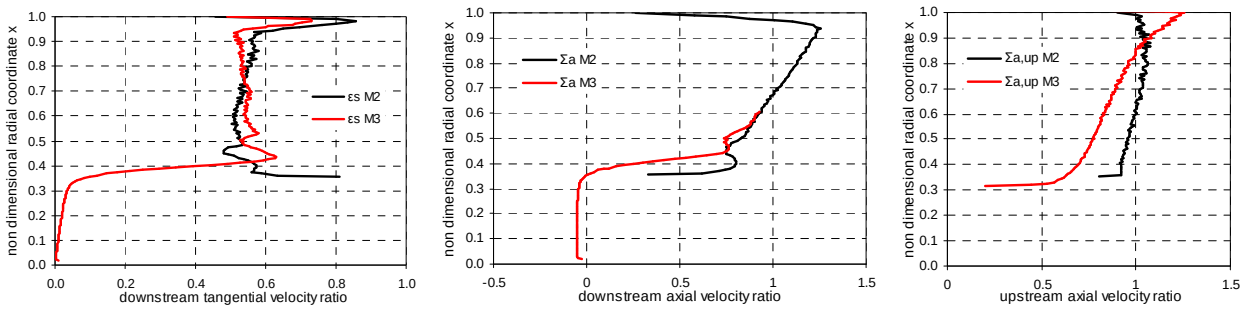

Figure 7. Velocity ratios: Tangential (left) and axial (middle) downstream to blades, axial (right) upstream to blades

CONCLUSIONS

A numerical assessment of a rotor-only low boss ratio axial fan performance with validation on experimental data was presented. The paper shows that when the analysis is carried out at the maximum level of detail, more than 1,500,000 cells are needed to get reliable results for each fluid volume containing the impeller blade channel.

When, instead, industrial applications are considered:

- Meshes with 600,000 cells are acceptable when two-equations one-layer turbulence models are used, the two-layers ones requiring 200,000 additional cells.

- Fan performance and efficiency are underestimated by extremely detailed geometrical models of the blade channel that overestimate frictional losses.

- Precise predictions of fan performance are obtained by the idealized meridional blade channel calculations when the blade tip clearance is considered in the model, also because of the counter-acting effects of the excessive dissipation predicted at blade tip and the idealized geometry.

- The numerical prediction of the flow field immediately upstream and downstream of the rotating blades is very sensitive to the degree of idealization of the meridional geometry. Thus, a detailed

description of all important geometrical features of fan is required for a detailed blading design analysis, although it leads to a less precise prediction of total fan performance parameters.

- Rough grid models of the entire fan (about 200,000 cells in the fluid volume surrounding the rotor) including all the geometric features and the realizable k-ε turbulence model, underestimate the total fan performance but predict with sufficient accuracy both the total efficiency and the trend of the characteristic curve also in the unstable operating zone.

ACKNOWLEDGEMENTS

Auhtors gratefully acknowledge Federica dalla Noce, executive chief of F.lli Ferrari Ventilatori S.p.A. Industrial Fan Technology. A special thank to Costantino Mogentale and Daniele Cariolato for their precious experimental testing activity.

REFERENCES

[1] Cumpsty N. C. - *Compressor aerodynamics, Longman Scientific &Technical*, **1989**

[2] Lakshminarayana B. - *Fluid dynamics and heat transfer of turbomachinery, Wiley, New York*, **1995**

[3] Stockman N. O., Kramer J. L. - *Method for design of pump impellers using a high-speed digital computer, NASA TN D-1562*, **1963**

[4] Novak, R. A. - *Streamline curvature computing procedures for fluid-flow problems, ASME J. Eng. Power, 89: 478–490*, **1967**

[5] McNally W. D., Sockol P. M. - *Computational methods for internal flows with emphasis on turbomachinery, NASA TM 82764*, **1981**

[6] Lin B. J., Hung C. I., Tang E. J. - *An optimal design of axial-flow fan blades by the machining method and an artificial neural network, PIME Part C, Vol 216*, **2002**

[7] Li Y., Liu J., Ouyang H., Du Z.H. - *Internal flow mechanism and experimental research of low pressure axial fan with forward-skewed Blades, Jounal of Hydrodynamics, 20(3):299-305*, **2008**

[8] Cho C. H., Cho S. Y., Ahn K. Y., Kim Y. C. - *Study of an axial-type fan design technique using an optimization method, PIME Part E, 223: 101*, **2009**

[9] Corsini A., Rispoli F., Sheard A. G. - *Shaping of tip end-plate to control leakage vortex swirl in axial flow fans, Journal of Turbomachinery, ASME, Vol. 132 / 031005-1*, **2010**

[10] UNI EN ISO 5801:2009 - *"Ventilatori industriali - Prove prestazionali su circuito normalizzato" (in Italian)*, **2009**

[11] Shih, T.H., Liou, W.W., Shabbir, A., Yang Z., Zhu J.- *A new $k-\varepsilon$ eddy viscosity model for high Reynolds number turbulent flow, Computer Fluids, 24(3):227-238*, **1995**

[12] Wolfstein M. - *The velocity and temperature distribution in one-dimensional flow with turbulence augmentation and pressure gradient, Int. J. Heat Mass Transfer, 12:301-318*, **1969**

[13] Kahane A. - *Investigation of axial-flow fan and compressor rotors designed for three-dimensional flow, NACA TN-1652*, **1948**

[14] Wallis R. A. - *Axial Flow Fans and Ducts, Krieger Publishing, Malabar, FL*, **1993**

[15] Downie R. J., Thompson M. C., Wallis R. A. – *An engineering approach to blade designs for low to medium pressure rise rotor-only axial fans, Experimental Thermal and Fluid Science, 6:376-401*, **1993**

© Massimo Masi, Andrea Lazzaretto